

General Disclaimer

One or more of the Following Statements may affect this Document

- This document has been reproduced from the best copy furnished by the organizational source. It is being released in the interest of making available as much information as possible.
- This document may contain data, which exceeds the sheet parameters. It was furnished in this condition by the organizational source and is the best copy available.
- This document may contain tone-on-tone or color graphs, charts and/or pictures, which have been reproduced in black and white.
- This document is paginated as submitted by the original source.
- Portions of this document are not fully legible due to the historical nature of some of the material. However, it is the best reproduction available from the original submission.

Final Report of the
NASA Contract NAS 9-9270

March 11, 1970

Part III

INVESTIGATION OF
ARCSINE DEVICES FOR PHASE
MODULATION PRODUCT DETECTOR APPLICATIONS

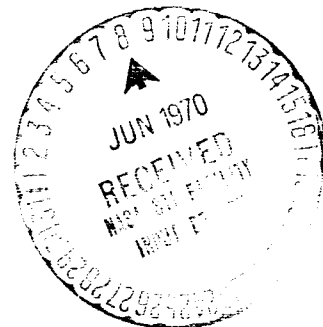
Prepared
by
N. M. Shehadeh
and
Russell H. Pacey, Jr.

FACILITY FORM 602

N70-28542
(ACCESSION NUMBER)
57
(PAGES)
CR-108452
(NASA CR OR TMX OR AD NUMBER)

(THRU)

(CODE)
10
(CATEGORY)



Final Report of the
NASA Contract NAS 9-9270

March 11, 1970

Part III

INVESTIGATION OF
ARCSINE DEVICES FOR PHASE
MODULATION PRODUCT DETECTOR APPLICATIONS

Prepared

by

N. M. Shehadeh

and

Russell H. Pacey, Jr.

ABSTRACT

Functional models capable of performing the arcsine function are investigated for possible application to phase modulation receivers utilizing product detection. A mathematical model of one of these functional models is developed, and its performance in terms of output versus input signal-to-noise ratio is investigated.

Modulation by a single sinusoid is considered for the case of an additive, white, Gaussian noise process, and both analytical and computer simulation techniques are utilized in determining the performance characteristics of the model. It is shown that the analytical results are valid for only a very limited case.

Results from the computer simulation indicate that for the model to be of any practical worth, the modulation index must be small while input signal-to-noise ratio must be relatively high.

TABLE OF CONTENTS

CHAPTER

I.	INTRODUCTION.....	1
II.	MATHEMATICAL MODELS FOR THE ARCSINE FUNCTION....	6
III.	ANALYTICAL RESULTS FOR SIGNAL-TO-NOISE RATIO PERFORMANCE.....	16
IV.	DEFINITION OF THE MODEL FOR DIGITAL COMPUTER SIMULATION.....	28
V.	RESULTS AND CONCLUSIONS.....	39
	REFERENCES.....	48
	APPENDIX A. LISTING OF COMPUTER PROGRAM USED FOR SIMULATION.....	49

LIST OF ILLUSTRATIONS

FIGURE		Page
1.	Phase-locked Loop PM Receiver.....	2
2.	Piecewise Linear Approximation Model for Arcsine Function.....	7
3.	Implementation of Taylor's Series Approximation of Arcsine Function.....	8
4.	Feedback Model for Arcsine Function.....	10
5.	Mathematical Model for Arcsine Device.....	12
6.	Alternate Method of Implementing Arcsine Model of Figure 5.....	13
7.	Implementation of Arcsine Device in Product Detector of PM Receiver.....	17
8.	Signal Spectrum and Noise Spectrum.....	19
9.	In-phase and Quadrature Components of a PM Signal Plus Noise.....	22
10.	Mathematical Model of Arcsine Device Used for Computer Simulation.....	29
11.	Input versus Output SNR for Arcsine Device for Modulation Index of 1.5.....	41
12.	Input versus Output SNR for Arcsine Device for Modulation Index of 0.3.....	42
13.	Difference in Output SNR Between Theoretical and Computer Simulation Results As a Function of Modulation Index for 100 DB of Input SNR....	45

CHAPTER I

INTRODUCTION

Communications systems employing phase modulation (PM) have attracted considerable interest in recent years, especially for application in the aerospace field. Of the several types of demodulation schemes available for use in PM receivers, product detectors utilizing phase-locked loops are of primary interest due to the relative ease of implementation, and because the output versus input signal-to-noise ratio (SNR) characteristics are essentially linear throughout the range of usable input signal-to-noise ratios (i.e., no threshold effects).

The performance of phase-locked loop product detectors in PM communications system receivers has been analyzed in detail by several authors (Teasdale, 1969; Painter and Hondros, 1966; Viterbi, 1966) with the help of certain assumptions which reduce the problem to an analysis of a linear system. A brief discussion of these techniques and results will serve to illustrate the assumption and introduce the problem to be considered in this study.

Figure 1 depicts a simplified block diagram of a typical product detector, with the input shown as a PM signal, $e_{IN} = A \sin [\omega_c t + \phi_m(t)]$, where:

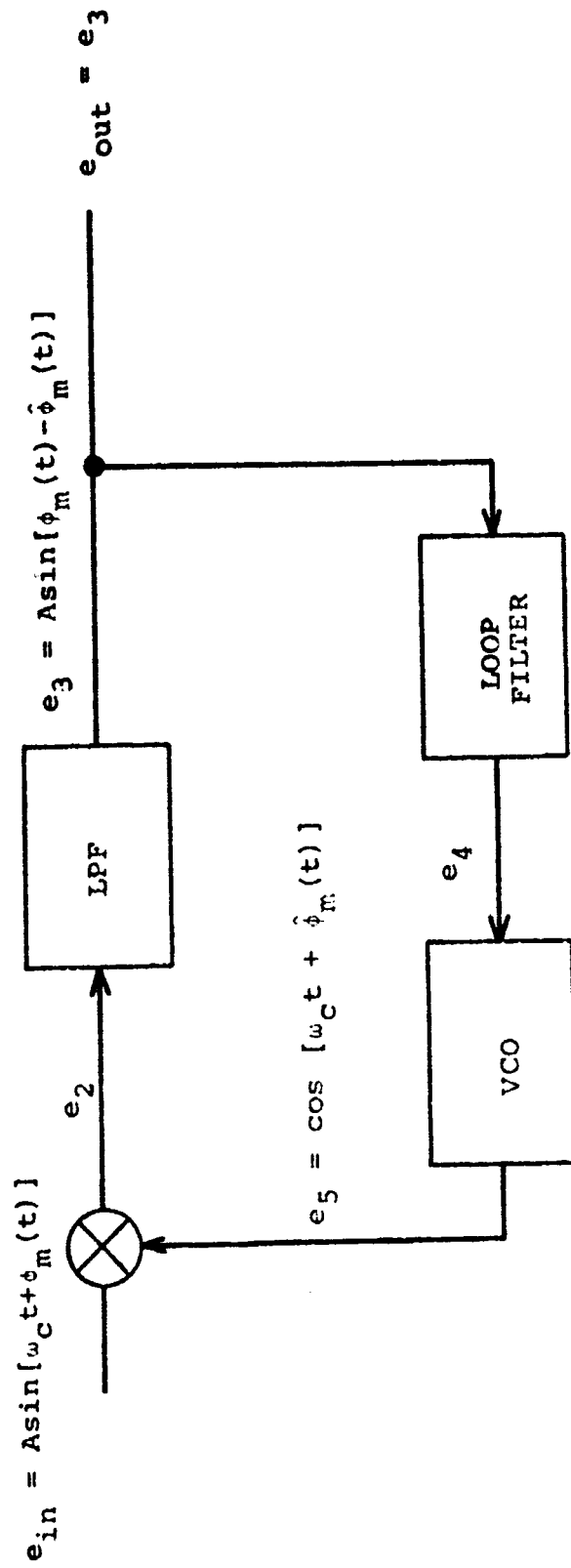


FIGURE 1. Phase-locked Loop PM Receiver

ω_c = radian frequency

$\phi_m(t)$ = phase modulation process

The voltage-controlled oscillator (VCO) is assumed to be free running at a radian frequency of ω_c , and in phase quadrature with the input signal e_{IN} . Thus, the output of the product device is:

$$\begin{aligned} e_2 &= A \sin [\omega_c t + \phi_m(t)] \cdot \cos[\omega_c t + \hat{\phi}_m(t)] & (1) \\ &= \frac{A}{2} \sin [2\omega_c t + \phi_m(t) + \hat{\phi}_m(t)] \\ &\quad + \frac{A}{2} \sin [\phi_m(t) - \hat{\phi}_m(t)] \end{aligned}$$

where $\hat{\phi}_m(t)$ = loop estimate of the PM process.

The low-pass filter (LPF) is assumed to have a pass-band such that the double frequency term is filtered out while the difference term is passed. Thus, the input to the loop filter is:

$$e_3 = \frac{A}{2} \sin [\phi_m(t) - \hat{\phi}_m(t)] \quad (2)$$

and $[\phi_m(t) - \hat{\phi}_m(t)]$ is defined as the relative phase error. Now, the output of the loop filter, e_4 , ideally should be a signal such that the modulation imposed on the VCO is exactly $\phi_m(t)$, so that the loop would operate with zero phase error. That is,

$$e_4 = \int \phi_m(t) dt$$

since the VCO in a frequency modulation (FM) device. For this to be the case, the loop filter would obviously have to be a non-linear device. However, if the phase error is at all times small compared to 1 radian, a simplifying

assumption may be made. That is;

$$e_3 = \frac{A}{2} \sin [\phi_m(t) - \hat{\phi}_m(t)] = \frac{A}{2} [\phi_m(t) - \hat{\phi}_m(t)] \quad (3)$$

In this case, the loop filter would be a simple integrator, and the system could be approximated as linear. However, this assumption places the restriction on the system that the phase variation be small, or, in other words, that the modulation index must be small compared to 1 radian. This is normally the case in practice.

If the use of modulation indices on the order of 1 radian is desired, it is seen that the loop filter must perform the arcsine function plus integration. That is, for an input of $\sin [x(t)]$, the filter must produce an output proportional to $\int x(t)dt$. In this case, the overall operation of the phase-locked loop product detector becomes linear, and it is possible to produce an output which is exactly proportional to the input PM process.

The purpose of this study is to develop a model which will perform the arcsine function for a single sinusoidal input signal, and to analyze the performance of this model when band-limited, white, Gaussian noise is present at the input. Specifically, it is desired to determine the output versus input SNR characteristics of such a model and special attention is directed to the threshold effects, if any. For purposes of analysis, the modulating signal will be assumed as a single sinusoidal signal.

In chapter II, a mathematical model is developed which will perform the arcsine function for a single sinusoidal input. Chapter III presents an analytical approach to developing the output SNR characteristics under the assumption of high input SNR, and discusses the results. Inasmuch as the model represents a nonlinear transfer function, no general results could be obtained by analytical methods, so a digital computer (SDS Sigma 7) was employed to simulate the model. The assumptions, theory developments, and techniques necessary for this approach are contained in Chapter IV. In Chapter V, results of the study are summarized, and conclusions are drawn concerning the techniques used to analyze the model, as well as probable performance of the model when implemented in a phase-lock loop product detector.

CHAPTER II

MATHEMATICAL MODELS FOR THE ARCSINE FUNCTION

In developing a mathematical model, or a system, to perform the arcsine function, one might consider several different approaches. Inasmuch as the basic requirements are that the system accept as input a function, $x(t)$, which is a sinusoid whose argument is some function of time,

$$x(t) = A \sin[\theta(t)] \quad (4)$$

and provide as output, $y(t)$, the argument of the input,

$$y(t) = \theta(t) \quad (5)$$

the system must obviously be non-linear for exact results.

However, adequate results may very well be obtained by a piecewise linear approximation of the arcsine function, consisting of two, three, or more segments. This concept is shown in Figure 2 for three segments. This system could be implemented relatively easily, using three linear amplifiers with appropriate gains, and a threshold device for selecting the proper amplifier, depending on the level of the input signal. Another approximation method which in theory would be more accurate consists of approximating the arcsine function by a truncation of the corresponding Taylor's series. This series is given by

$$\arcsine(x) = x + \frac{1 \cdot x^3}{2 \cdot 3} + \frac{1 \cdot 3 \cdot x^5}{2 \cdot 4 \cdot 5} + \frac{1 \cdot 3 \cdot 5 \cdot x^7}{2 \cdot 4 \cdot 6 \cdot 7} + \dots \quad (6)$$

and an approximation consisting of the first four terms of

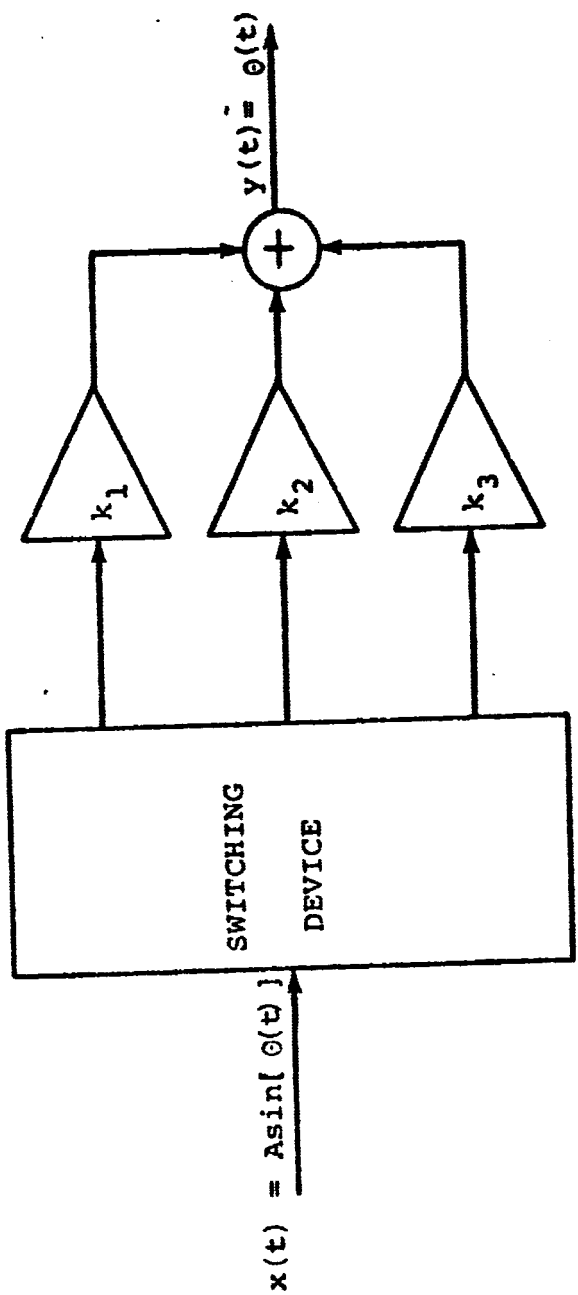


FIGURE 2. Piecewise Linear Approximation Model for Arcsine Function

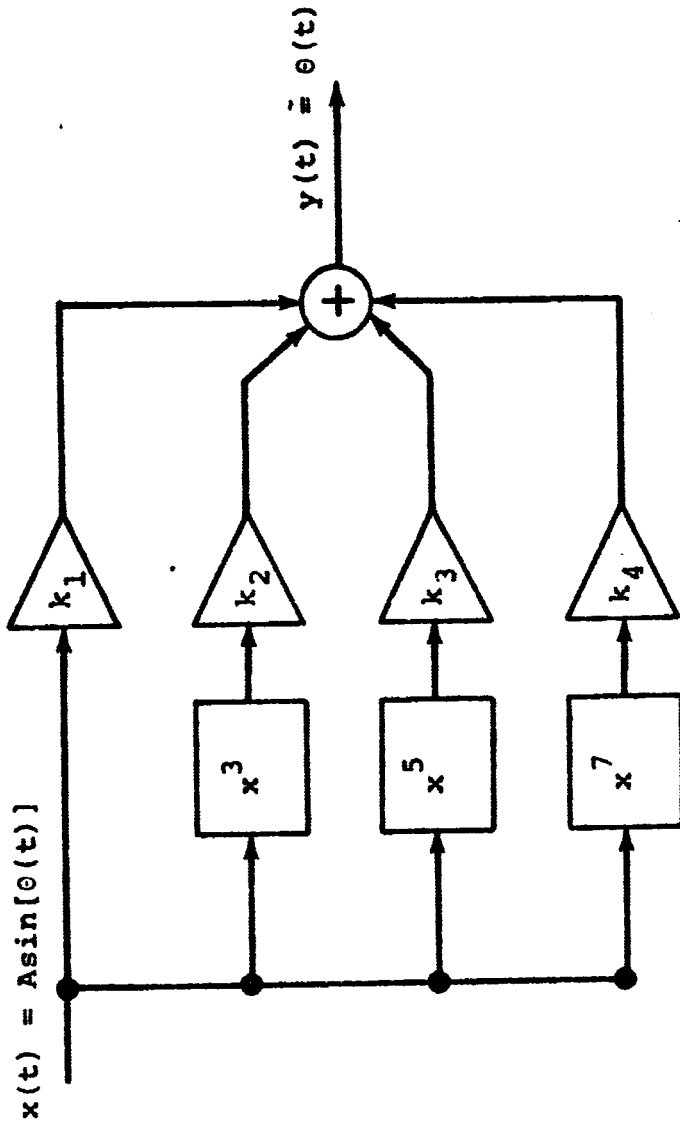


FIGURE 3. Implementation of Taylor's Series Approximation of Arcsine Function

(6) could be implemented as shown in Figure 3. In practice, it would probably be difficult to obtain accurate devices for the cubic and higher terms.

Alternatively, a method utilizing an operational amplifier and a sinusoidal function generator could be used which would provide excellent accuracy. The connection of these devices is shown in Figure 4, and the closed loop equation for system operation is:

$$\{x(t) - \sin [y(t)]\}K = y(t) \quad (7)$$

Rearrangement of terms leads to:

$$\sin [y(t)] = \frac{Kx(t) - y(t)}{K} \quad (8)$$

If the gain of the operational amplifier is very large this equation reduces to:

$$\sin [y(t)] = x(t) \quad (9)$$

or, solving for $y(t)$,

$$y(t) = \arcsine[x(t)] \quad (10)$$

and $y(t) = \theta(t)$

All of the preceding methods approximate a true arcsine; that is, regardless of the input, the output is the arcsine of the input. This has one potential drawback in that the input must be amplitude limited to ± 1 volt for proper system operation.

The model developed for further study in this thesis differs from the other methods in that it performs the arcsine function only for sinusoidal inputs. The derivation is

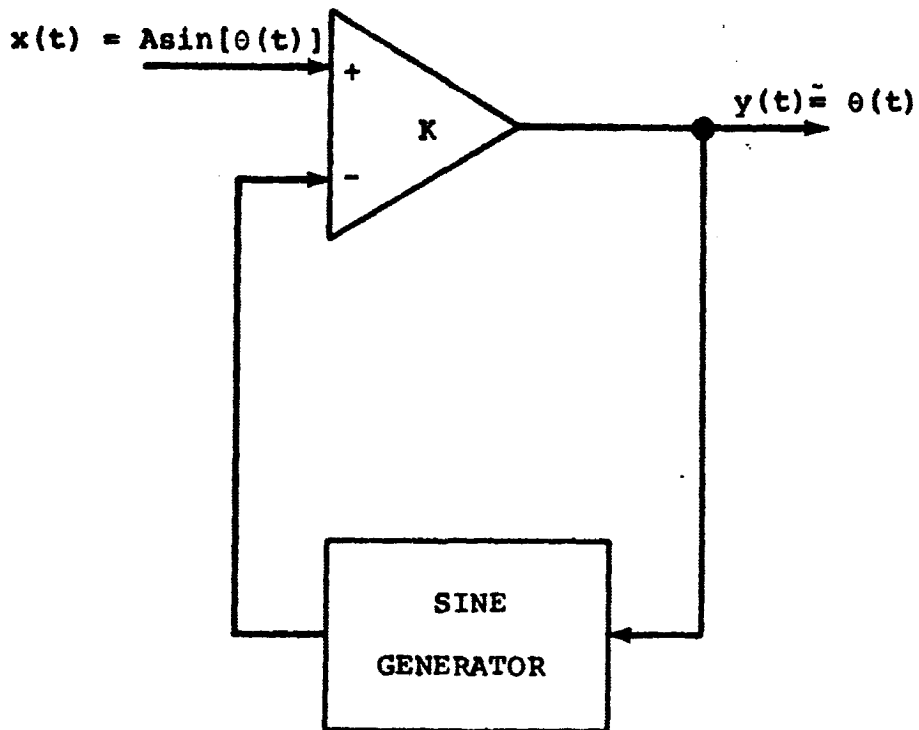


FIGURE 4. Feedback Model for Arcsine Function

based on the observation that differentiation of the input sinusoid with respect to time results in a signal which is amplitude modulated by the derivative of the PM process.

That is, if the input signal is;

$$x(t) = A \sin [\theta(t)]$$

then,

$$\frac{dx(t)}{dt} = A \frac{d\theta(t)}{dt} \cdot \cos[\theta(t)] \quad (11)$$

However, conventional AM demodulation schemes could not be used due to the lack of frequency separation in the modulating signal and the "carrier". Therefore, a division process was devised whereby the original input signal is shifted in phase by 90 degrees and divided into the differentiated signal. Integration of the resulting signal produces the desired output. A diagram of this mathematical model is shown in Figure 5, where the 90 degree phase shift is implemented as a quadrature filter, which has an impulse response of $\frac{1}{\pi t}$.

An alternative method of implementing this mathematical model is shown in Figure 6. The closed loop equation for this system is:

$$\{\theta'(t)A\cos[\theta(t)] - Z(t)A\cos[\theta(t)]\}K = Z(t) \quad (12)$$

Rearranging terms,

$$Z(t)[AK\cos[\theta(t)] - 1] = \theta'(t)AK\cos[\theta(t)] \quad (13)$$

and, for large K, this simplifies to;

$$Z(t) = \theta'(t) \quad (14)$$

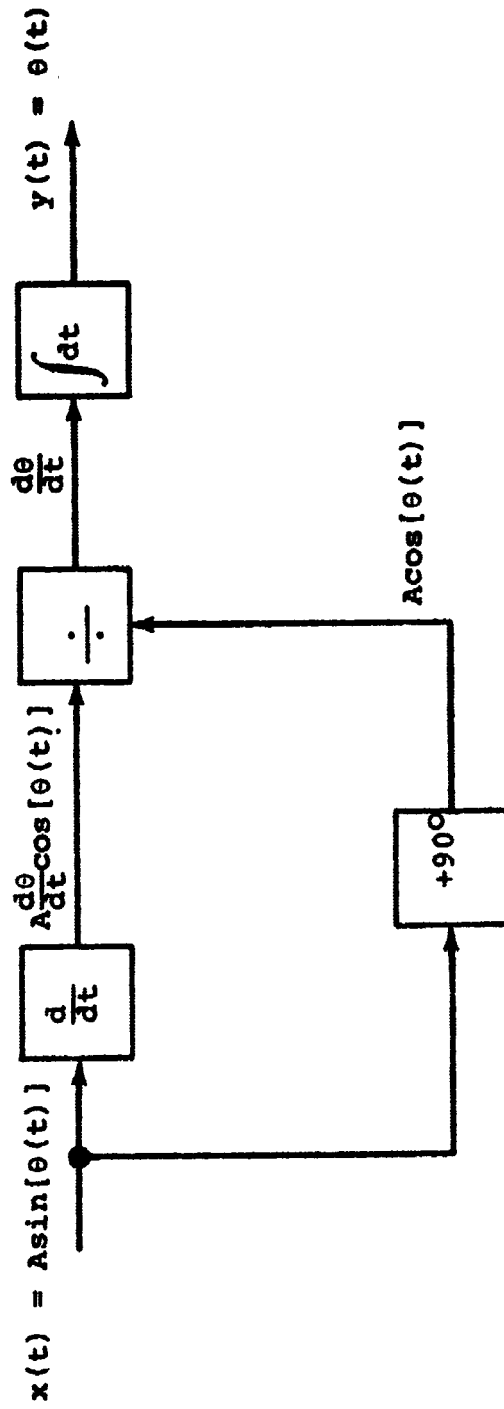


FIGURE 5. Mathematical Model of Arcsine Device

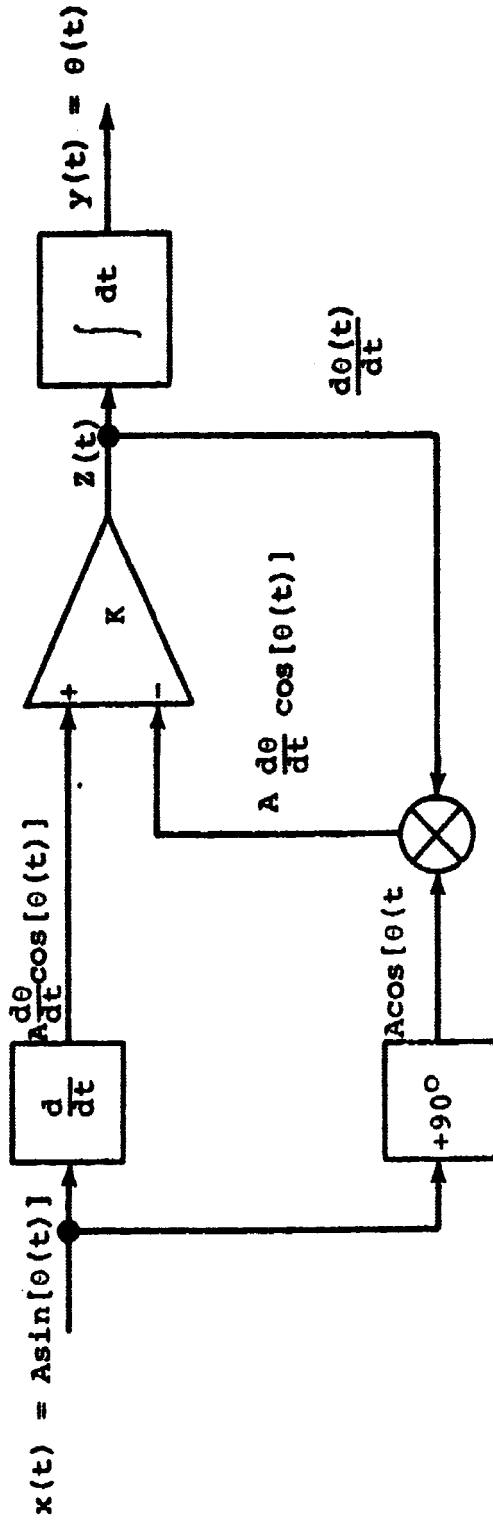


FIGURE 6. Alternate Method of Implementing Arcsine Model of Figure 5.

Therefore, the output is;

$$y(t) = \int Z(t)dt = \theta(t) \quad (15)$$

Returning to the model of Figure 5, and assuming the input consists of signal, $s(t)$, plus noise, $n(t)$, the output of the divider is seen to be;

$$Z(t) = \frac{s'(t) + n'(t)}{\hat{s}(t) + \hat{n}(t)} \quad (16)$$

$$\text{where } s'(t) = \frac{ds(t)}{dt} \quad \hat{s}(t) = s(t) * \frac{1}{\pi t}$$

$$n'(t) = \frac{dn(t)}{dt} \quad \hat{n}(t) = n(t) * \frac{1}{\pi t}$$

Since the signal portion of $Z(t)$ is known to be $\theta'(t)$, the noise portion of the voltage must be;

$$n_1(t) = Z(t) - \theta'(t) \quad (17)$$

Substituting for $Z(t)$ from Equation (16);

$$n_1(t) = \frac{s'(t) + n'(t)}{\hat{s}(t) + \hat{n}(t)} - \theta'(t) \quad (18)$$

$$= \frac{s'(t) + n'(t) - \hat{s}(t) \cdot \theta'(t) - \hat{n}(t) \cdot \theta'(t)}{\hat{s}(t) + \hat{n}(t)}$$

Now, since;

$$s(t) = A \sin[\theta(t)]$$

$$\hat{s}(t) = A \cos[\theta(t)]$$

$$s'(t) = A[\theta'(t)]\cos[\theta(t)]$$

it follows that;

$$s'(t) = \hat{s}(t) \cdot \theta'(t) \quad (19)$$

and, thence;

$$n_1(t) = \frac{n'(t) - \hat{n}(t) \cdot \theta'(t)}{\hat{s}(t) + \hat{n}(t)} \quad (20)$$

* is used to indicate convolution

Then, the noise at the output of the system would be;

$$n_o(t) = \int n_1(t)dt \quad (21)$$

However, due to the nonlinear characteristics of Equation (20), it is impossible to obtain a general closed form expression for the output noise, or a quantitative measure of output noise power as a function of input noise power by conventional analytical techniques. The remainder of this manuscript is devoted to methods of approximating these quantities, and the following chapter presents analytical results for the special case of high input signal-to-noise ratio.

CHAPTER III

ANALYTICAL RESULTS FOR SIGNAL-TO-NOISE
RATIO PERFORMANCE

Although it is desirable to obtain general, exact analytical results for the signal-to-noise ratio (SNR) performance characteristics of the arcsine device, it is felt that this is, in general, an impossible task, due to the inherent nonlinear properties of such a system.

It is important to note that the arcsine model proposed for this study is a true arcsine only for a single sinusoidal input, and not for a general, unspecified input. Thus, for a single sinusoidal input it is known that the system output will be the argument of that sinusoidal input, however, for any other input, the output will not, in general be the arcsine of the input, and therefore, the transfer function of the system cannot be uniquely specified, but depends on the nature of the input. This heuristic argument leads to the conclusion that it is not possible to apply an analytical approximation method to the general case noise analysis for the purpose of obtaining a closed form approximate result.

However, for the special case of high input SNR, it is possible to obtain approximate results for the output versus input SNR characteristics of the system. It is assumed the arcsine device is implemented in a product

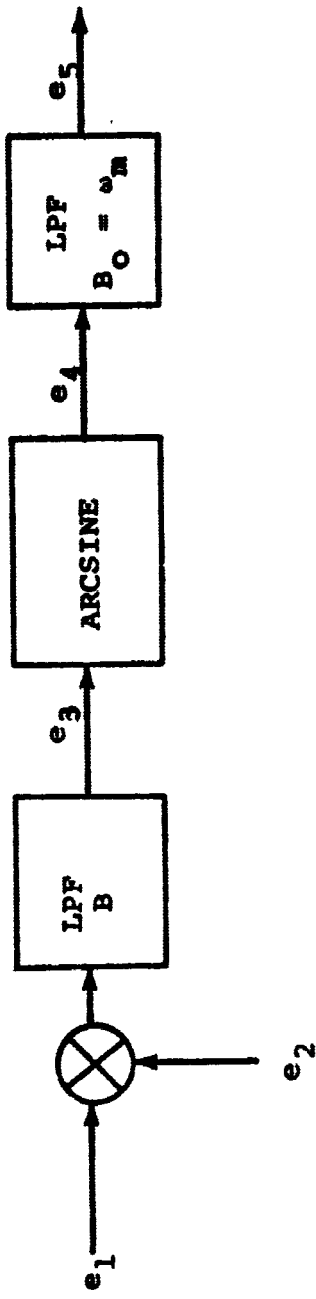


FIGURE 7. Implementation of Arcsine Device in Product Detector of PM Receiver

detector as depicted in Figure 7, and that the following general assumptions can be made regarding the system:

- (1) The input voltage, e_1 , is the sum of a phase modulated sinusoid carrier at ω_c rad/sec, and white, Gaussian noise with spectral density N_0 watts per cycle of frequency.
- (2) The input frequency spectrum has been limited to a band of ω_0 rad/sec centered about the carrier frequency, where $\omega_c \gg \omega_0$, and that this band is sufficiently wide to accommodate all of the input signal components down to 1% or less relative magnitude, as shown in Figure 8A.
- (3) Modulation of the carrier is by a single sinusoid, $\phi_m(t) = \beta \sin \omega_m t$, where β is the modulation index, and ω_m is the modulating frequency.
- (4) The ratio of input signal power to average input noise power is high.
- (5) All filters are ideal.

The input voltage, e_1 , can then be written as;

$$e_1 = A \sin(\omega_c t + \beta \sin \omega_m t) + n(t) \quad (22)$$

where $n(t)$ = sample function from the input Gaussian noise process, and

A = carrier amplitude

For the narrow-band Gaussian noise process under consideration here, it has been shown (Davenport and Root,

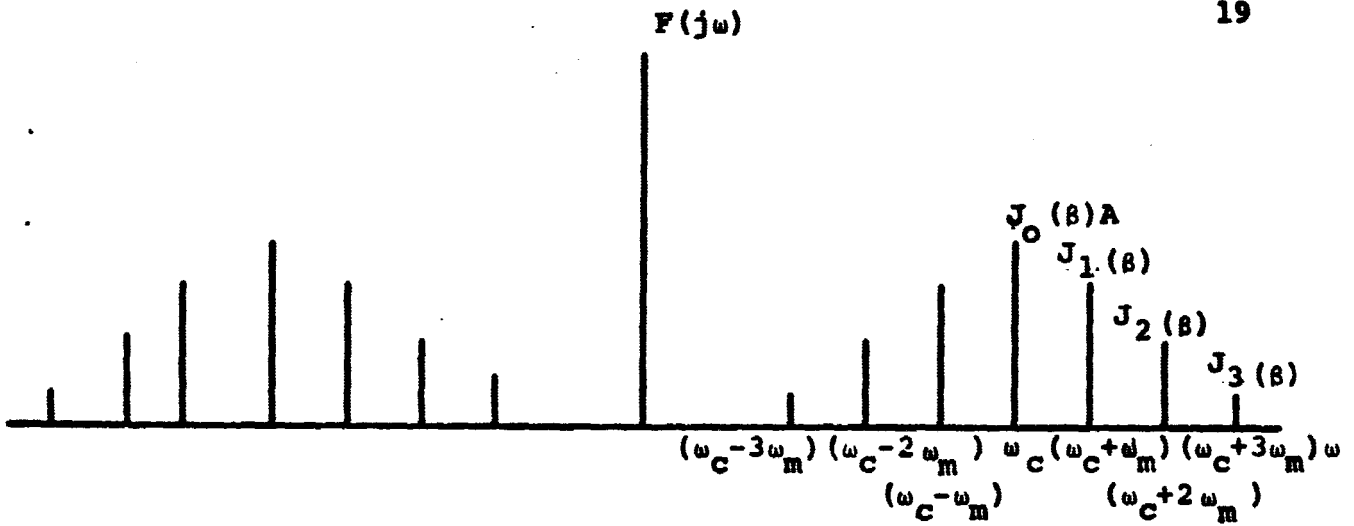


FIGURE 8A. Signal Spectrum

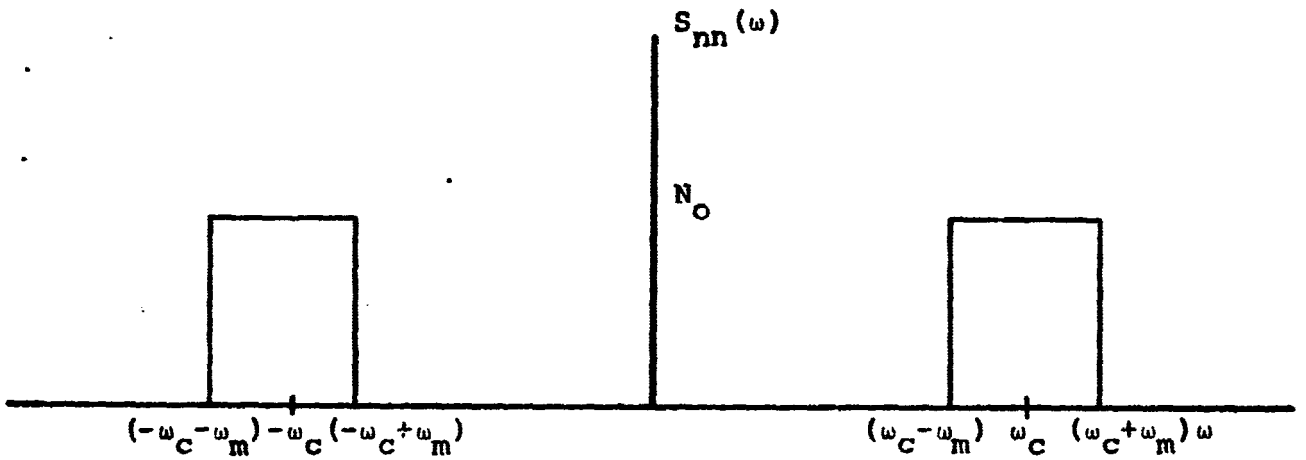


FIGURE 8B. Noise Spectrum

1958; Bennett, 1960) that the sample function, $n(t)$, can be expressed as;

$$n(t) = x(t) \cdot \cos \omega_c t - y(t) \cdot \sin \omega_c t \quad (23)$$

and, furthermore, that $x(t)$ and $y(t)$ are sample functions of independent Gaussian processes, where;

$$E\{x(t)\} = E\{y(t)\} = E\{n(t)\} = 0 \quad (24)$$

$$E\{x^2(t)\} = E\{y^2(t)\} = E\{n^2(t)\} = \sigma_n^2 \quad (25)$$

where $E\{\cdot\}$ = expected value of term in brackets.

In addition, if the power spectral densities of $n(t)$, $x(t)$, and $y(t)$ are $S_{nn}(\omega)$, $S_{xx}(\omega)$, and $S_{yy}(\omega)$, respectively, then;

$$S_{xx}(\omega) = S_{yy}(\omega) = S_{nn}(\omega + \omega_c) + S_{nn}(\omega - \omega_c) \quad (26)$$

Now, for noise of constant spectral density (or more simply, "white" noise), it is obvious that the spectrum of $n(t)$ will be as shown in Figure 8B, and that;

$$\begin{aligned} S_{nn}(\omega) &= N_0 & \omega_c - \frac{\omega_0}{2} \leq |\omega| \leq \omega_c + \frac{\omega_0}{2} \\ &= 0 & \text{otherwise} \end{aligned} \quad (27)$$

Therefore, the total average input noise power to the system of Figure 7 will be;

$$\begin{aligned} P_n &= \frac{1}{2\pi} \int_{-\infty}^{\infty} S_{nn}(\omega) d\omega \\ P_n &= 2N_0 f_0 \end{aligned} \quad (28)$$

and the input signal power will be;

$$P_s = A^2/2 \quad (29)$$

Equations (28) and (29) yield the input signal-to-noise ratio as;

$$\text{SNR}_i = \frac{A^2}{4N_0T_0} \quad (30)$$

Equations (22) and (23) may be combined to yield;

$$\begin{aligned} e_1 &= A\sin(\omega_c t + \beta \sin \omega_m t) + x(t) \cdot \cos \omega_c t - y(t) \cdot \sin \omega_c t \\ &= A\sin \omega_c t \cdot \cos(\beta \sin \omega_m t) + A\cos \omega_c t \cdot \sin(\beta \sin \omega_m t) \\ &\quad + x(t) \cdot \cos \omega_c t - y(t) \cdot \sin \omega_c t \end{aligned} \quad (31)$$

Factoring results in ;

$$\begin{aligned} e_1 &= [A\cos(\beta \sin \omega_m t) - y(t)] \cdot \sin \omega_c t \\ &\quad + [A\sin(\beta \sin \omega_m t) + x(t)] \cdot \cos \omega_c t \end{aligned} \quad (32)$$

Thus, e_1 is the vector sum of two quadrature vectors whose amplitudes are time varying, as shown in Figure 9, and this vector sum may be replaced by the appropriate single vector whose form is;

$$e_1 = R(t) \cdot \sin[\omega_c t + \theta(t)] \quad (33)$$

The amplitude, $R(t)$, and phase, $\theta(t)$, of this resulting vector will then be;

$$R(t) = \sqrt{[A\cos(\beta \sin \omega_m t) - y(t)]^2 + [A\sin(\beta \sin \omega_m t) + x(t)]^2} \quad (34)$$

$$\theta(t) = \arctan \left(\frac{A\sin(\beta \sin \omega_m t) + x(t)}{A\cos(\beta \sin \omega_m t) - y(t)} \right) \quad (35)$$

Now for the assumed conditions of high input SNR, the amplitude function, $R(t)$, becomes approximately;

$$R(t) = \sqrt{A^2 \cos^2(\beta \sin \omega_m t) + A^2 \sin^2(\beta \sin \omega_m t)} \quad (36)$$

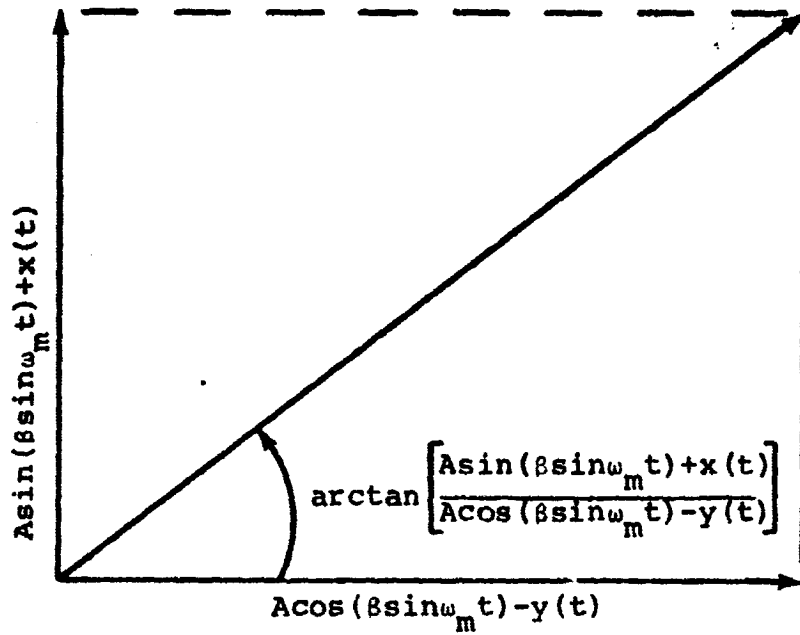


FIGURE 9. In-phase and Quadrature Components of a PM Signal Plus Noise

or, $R(t) = A$ for $A^2/2 \gg E\{y^2(t)\}$

The Taylor series expansion for a function of two variables about the point (0,0) is;

$$f(u,v) = f(0,0) + uf_u(0,0) + vf_v(0,0) + \frac{1}{2!} [u^2 f_{uu}(0,0) + 2uv f_{uv}(0,0) + v^2 f_{vv}(0,0)] + \dots$$

where f_u, f_v denote partial derivatives with respect to u, v , etc. If $\theta(t)$ is expanded in this manner in terms of $x(t)$ and $y(t)$, and only the linear terms are retained, the result is;

$$\theta(t) = \arctan \left(\frac{A \sin(\beta \sin \omega_m t)}{A \cos(\beta \sin \omega_m t)} \right) + \frac{\frac{x(t)}{A \cos(\beta \sin \omega_m t)}}{1 + \frac{A^2 \sin^2(\beta \sin \omega_m t)}{A^2 \cos^2(\beta \sin \omega_m t)}} - \frac{\frac{y(t) \cdot A \sin(\beta \sin \omega_m t)}{A^2 \cos^2(\beta \sin \omega_m t)}}{1 + \frac{A^2 \sin^2(\beta \sin \omega_m t)}{A^2 \cos^2(\beta \sin \omega_m t)}}$$

Use of trigonometric identities yields;

$$\theta(t) = \beta \sin \omega_m t + \frac{x(t)}{A} \cos(\beta \sin \omega_m t) - \frac{y(t)}{A} \sin(\beta \sin \omega_m t) \quad (37)$$

Since the assumption of high input SNR requires that;

$$\frac{x(t)}{A} ; \frac{y(t)}{A} \ll 1$$

the second order terms which involve $x^2(t)/A^2$ and $y^2(t)/A^2$ may be neglected as a good approximation. Therefore, the input signal to the system in Figure 7 is given, to a good approximation, by;

$$e_1 = A \sin[\omega_c t + \theta(t)] ,$$

where $\theta(t)$ is given by Equation (37).

As was shown in Chapter 1, the out put of the low pass filter following the product device is;

$$e_3 = \frac{A}{2} \sin[\theta(t)]$$

and, from results given in Chapter II, Equation (15), the output of the arcsine device will be;

$$e_4 = \theta(t) = \beta \sin \omega_m t + \frac{x(t)}{A} \cos(\beta \sin \omega_m t) - \frac{y(t)}{A} \sin(\beta \sin \omega_m t) \quad (38)$$

Therefore, the noise at this point is;

$$n_1(t) = \frac{x(t)}{A} \cos(\beta \sin \omega_m t) - \frac{y(t)}{A} \sin(\beta \sin \omega_m t) \quad (39)$$

It is important to note that although Equation (37) gives a good approximation to Equation (35) for high input SNR, Equation (39) is not necessarily a good approximation to the noise, since the premise used to obtain this approximation is that the noise is small compared to the signal. The potential pitfalls in using Equation (39) will be discussed later.

The total average power of a stochastic process is defined as;

$$P_{avg} = \frac{1}{2\pi} \int_{-\infty}^{\infty} S_{uu}(\omega) d\omega = R_{uu}(0) = E\{u^2(t)\} \quad (40)$$

where $R_{uu}(0)$ = autocorrelation function of $u(t)$

evaluated at zero.

So, the noise power at this point is;

$$P_{n1} = E\left\{\left[\frac{x(t)}{A} \cos(\beta \sin \omega_m t) - \frac{y(t)}{A} \sin(\beta \sin \omega_m t)\right]^2\right\}$$

$$P_{n1} = E\left\{\frac{x^2(t)}{A^2} \cos^2(\beta \sin \omega_m t)\right\} + E\left\{\frac{y^2(t)}{A^2} \sin^2(\beta \sin \omega_m t)\right\} \\ - 2E\left\{\frac{x(t) \cdot y(t)}{A^2}\right\} \cdot \cos(\beta \sin \omega_m t) \cdot \sin(\beta \sin \omega_m t) \quad (41)$$

Now, since $x(t)$ and $y(t)$ are independent processes, the use of Equation (24) yields;

$$E\{x(t) \cdot y(t)\} = E\{x(t)\}E\{y(t)\} = 0 \quad (42)$$

Using Equations (25) and (42) in Equation (41) yields;

$$P_{n1} = \frac{E\{x^2(t)\}}{A^2} [\cos^2(\beta \sin \omega_m t) + \sin^2(\beta \sin \omega_m t)] \\ = \frac{E\{x^2(t)\}}{A^2} \quad (43)$$

Also, from Equations (26) and (27);

$$S_{xx}(\omega) = 2N_0 \quad |\omega| \leq \frac{\omega_0}{2} \quad (44) \\ = 0 \quad \text{otherwise}$$

Thus, the noise spectral density at the arcsine device output is;

$$S_{n1n1}(\omega) = 2N_0/A^2 \quad |\omega| \leq \frac{\omega_0}{2} \quad (45) \\ = 0 \quad \text{otherwise}$$

Digressing for a moment to the question raised previously of the accuracy of the approximation to the noise which was necessary to obtain this result, it is possible to show one case for which the approximation is accurate. Again, assume high input SNR, and consider the limit of Equation (35) as β approaches zero;

$$\begin{aligned}
 \lim_{\beta \rightarrow 0} \theta(t) &= \lim_{\beta \rightarrow 0} \arctan \left(\frac{A \sin(\beta \sin \omega_m t) + x(t)}{A \cos(\beta \sin \omega_m t)} \right) \\
 &= \arctan \left(\frac{x(t)}{A} \right) \\
 &= \frac{x(t)}{A} \text{ for } \frac{x(t)}{A} \ll 1
 \end{aligned} \tag{46}$$

Therefore, for the case of no modulation and high SNR;

$$P_{n_1} = \frac{E\{x^2(t)\}}{A^2} \tag{47}$$

which agrees with Equation (43).

For other values of β , Equation (43) may or may not be valid, and this question is discussed at length in Chapter V, where results of this chapter are compared to computer simulation results.

Passing the noise through the output low-pass filter limits the noise spectrum to a bandwidth of ω_m rad/sec, and therefore the output noise spectral density is;

$$\begin{aligned}
 S_{n_0 n_0}(\omega) &= 2N_0/A^2 & |\omega| \leq \omega_m \\
 &= 0 & \text{otherwise}
 \end{aligned} \tag{48}$$

where it is assumed that $\omega_m < \omega_0/2$

Thus, the noise power at the output of the system is;

$$P_{n_0} = \frac{2N_0 f_m}{A^2} \tag{49}$$

The output signal voltage and power are;

$$\begin{aligned} s_o(t) &= \beta \sin \omega_m t \\ P_{s_o} &= \beta^2 / 2 \end{aligned} \quad (50)$$

Therefore, the output SNR, from Equations (49) and (50) is seen to be;

$$\text{SNR}_o = \frac{\beta^2 A^2}{4N_o f_m} \quad (51)$$

It has been shown (Batson, 1967) that the output SNR for an equivalent system without the arcsine device is given by:

$$\text{SNR} = \frac{A^2 J_1^2(\beta)}{2N_o f_m} \quad (52)$$

where $J_1(\beta)$ = first order Bessell function of β .

The following chapter presents the development of a computer simulation model for the arcsine device, which extends approximate results into the low input SNR region, and provides some insight into the variation of noise power as a function of the modulation index, β .

CHAPTER IV

DEFINITION OF THE MODEL FOR DIGITAL COMPUTER SIMULATION

Since the performance of the arcsine model proposed for this study could not be studied for the general case using analytical methods, a digital computer simulation routine was developed for the purpose of obtaining samples of the noise and digitally processing these samples to obtain an approximation of the output noise power. The computer program was written in the Fortran IV language, and the Scientific Data Systems' Sigma 7 was used to obtain solutions to the program.

The arcsine model used for the simulation is the same as described previously, with the exception that the output low-pass filter and the integrator have been interchanged as shown in Figure 10. Since these are both linear devices, this has no effect on the model output. Ideal devices have been assumed in all cases in the arcsine model.

The major problem in the simulation is developing a convenient and accurate method of describing the input noise voltage to the system. A random number generator with normal distribution was considered, but on further inspection it was found that this would require a prohibitively high number of calculations. The method used in

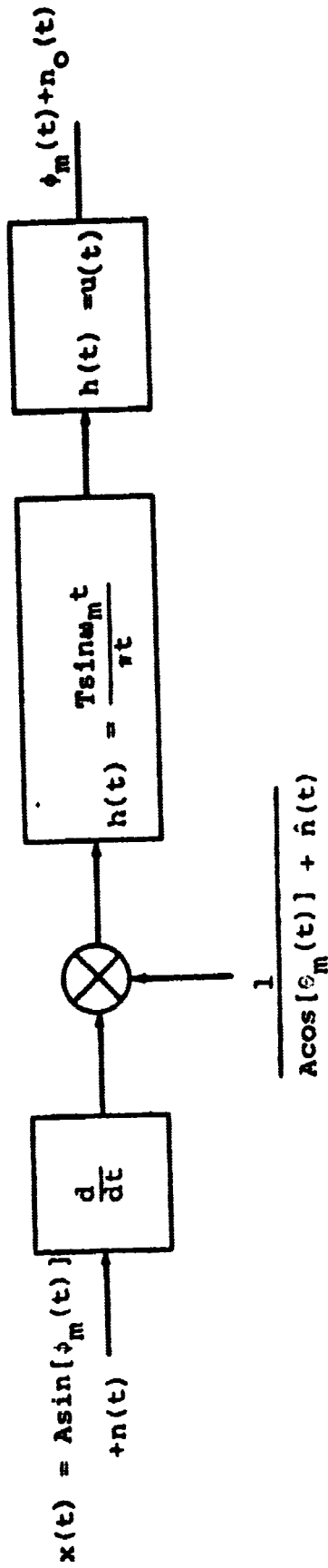


FIGURE 10. Mathematical Model of Arcsine Device Used for Computer Simulation

the program (Hancock, 1961) approximates white, bandlimited, Gaussian noise as a series of sinusoids spaced closely and evenly throughout the bandwidth.

$$n(t) = \sum_{k=1}^{B/\Delta f} \Delta n \cdot \sin\left[\frac{(2k-1)\Delta\omega t}{2}\right] \quad (53)$$

where B = input bandwidth in Hz

$\Delta f = \Delta\omega/2\pi$ = frequency spacing between adjacent terms in Hz

Δn = amplitude of each term

The power contained in $n(t)$ is;

$$P_n = \frac{(\Delta n)^2}{2} \cdot \frac{B}{\Delta f} \quad (54)$$

The average power of white Gaussian noise with two-sided spectral density, N_0 watts/Hz, in a band of B Hz is;

$$P_n = 2N_0 B \quad (55)$$

Equating these two to obtain Δn yields,

$$\begin{aligned} (\Delta n)^2 &= 4N_0 \Delta f \\ \Delta n &= 2\sqrt{N_0 \Delta f} \end{aligned} \quad (56)$$

The input to the arcsine model is assumed as noise, $n(t)$ defined as above, and signal, $s(t)$; where;

$$s(t) = A \sin [\phi_m(t)] \quad (57)$$

$$\phi_m(t) = \beta \sin\omega_m t$$

From Chapter II, Equation (20), the input noise to the low-pass filter is;

$$n_1(t) = \frac{n'(t) - \hat{n}(t) \cdot \phi'_m(t)}{\hat{s}(t) + \hat{n}(t)} \quad (58)$$

where $\phi'_m(t) = \beta \cdot \omega_m \cdot \cos \omega_m t$

$$\hat{s}(t) = A \cos(\beta \sin \omega_m t)$$

$$\hat{n}(t) = \frac{B/\Delta f}{\sum_{k=1}^{\infty}} 2\sqrt{N_0 \Delta f} \cos\left[\frac{(2k-1)}{2} \Delta \omega t\right], \text{ and}$$

$$n'(t) = \frac{B/\Delta f}{\sum_{k=1}^{\infty}} 2\sqrt{N_0 \Delta f} \cdot (2k-1) \Delta \omega / 2 \cdot \cos\left[\frac{(2k-1)}{2} \Delta \omega t\right]$$

Equation (58) is very adaptive to iterative computation, and thus samples of $n_1(t)$ may be easily obtained as a function of time.

As is well known, the output of a linear filter for a given input time function is simply the convolution of the impulse response, $h(t)$, of the filter with the time function, and this process is defined as,

$$f(t) * h(t) = \int_{-\infty}^{\infty} f(t-\tau)h(\tau)d\tau$$

The sampling theorem states that if a band-limited signal is sampled at a rate greater than twice the highest frequency, and the resultant samples are passed through an appropriate low-pass filter, the output will be an exact reproduction of the original time signal. Since the interest here is only in that portion of the noise which lies

within the bandwidth of the output low-pass filter, this same filter may be used to process noise voltage samples and reproduce that noise which is within the band of interest.

Thus, if samples of $n_1(t)$ are obtained using Equation (58), then $n_1(t)$ may be written as;

$$n_1(t) = \sum_{k=-\infty}^{\infty} A_k \delta(t-kT) \quad (59)$$

where T is the reciprocal of the sampling frequency, A_k is the noise voltage sample taken at $t=kT$, and $\delta(t-kT)$ is the Dirac delta function at $t=kT$

Since the impulse response of an ideal low-pass filter with bandwidth of ω_m rad/sec is given by;

$$h_1(t) = \frac{T \sin \omega_m t}{\pi t} \quad (60)$$

where T is the gain of the LPF as stated by the sampling theorem, the low-pass filter output is;

$$\begin{aligned} g(t) &= n_1(t) * h_1(t) = T \int_{-\infty}^{\infty} \sum_{k=-\infty}^{\infty} A_k \delta(t-kT-\tau) \frac{\sin \omega_m \tau}{\pi \tau} d\tau \\ &= \frac{T}{\pi} \sum_{k=-\infty}^{\infty} A_k \frac{\sin \omega_m (t-kT)}{(t-kT)} \end{aligned} \quad (61)$$

Now, the impulse response of an ideal integrator is given by;

$$h_2(t) = U(t) \quad (62)$$

where $U(t)$ is a unit step function.

Therefore, the system noise output is

$$n_o(t) = g(t) * h_2(t)$$

$$n_o(t) = \frac{T}{\pi} \sum_{k=-\infty}^{\infty} A_k \int_{-\infty}^{\infty} U(t-\tau) \frac{\sin \omega_m(\tau-kT)}{\tau-kT} d\tau$$

Letting $\omega_m(\tau-kT) = \alpha$

so that $d\tau = d\alpha/\omega_m$

$$\tau = \alpha/\omega_m + kT$$

$$n_o(t) = \frac{T}{\pi} \sum_{k=-\infty}^{\infty} A_k \int_{-\infty}^{\omega_m(t-kT)} \frac{\sin \alpha}{\alpha} d\alpha \quad (63)$$

$$\begin{aligned} \text{since } U(t-\alpha/\omega_m-kT) &= 1 \text{ for } \alpha < \omega_m(t-kT) \\ &= 0 \text{ for } \alpha > \omega_m(t-kT) \end{aligned}$$

Clearly, it is impossible to calculate $n_o(t)$ from Equation (63) as long as the summation is unbounded, unless the summation converges for both negative and positive k . Suppose that the summation is truncated to $\pm N$. Equation (63) then becomes;

$$\begin{aligned} n_o(t) &= \frac{T}{\pi} \sum_{k=-N}^N A_k \int_{-\infty}^{\omega_m(t-kT)} \frac{\sin \alpha}{\alpha} d\alpha \\ &= \frac{T}{\pi} A_{-N} \int_{-\infty}^{\omega_m(t+NT)} \frac{\sin \alpha}{\alpha} d\alpha + A_{-N+1} \int_{-\infty}^{\omega_m(t+NT-T)} \frac{\sin \alpha}{\alpha} d\alpha + \\ &\quad \dots + \frac{T}{\pi} A_0 \int_{-\infty}^{\omega_m t} \frac{\sin \alpha}{\alpha} d\alpha + \dots \end{aligned}$$

$$+ \frac{T}{\pi} A_{N-1} \int_{-\infty}^{\omega_m(t-NT+T)} \frac{\sin \alpha}{\alpha} d\alpha + \frac{T}{\pi} A_N \int_{-\infty}^{\omega_m(t-NT)} \frac{\sin \alpha}{\alpha} d\alpha \quad (64)$$

For some t , and a suitably large integer $N(NT \gg t)$, the integral in the last term in Equation (64) will approach zero, and therefore inclusion of additional terms, A_{N+1}, A_{N+2}, \dots , would have no significant effect on the final value of $n_0(t)$. Similarly, the first integral in the first term of Equation (64) approaches π , since;

$$\int_{-\infty}^{\infty} \frac{\sin x}{x} dx = \pi$$

Thus, if the A_k are periodic with index I , and have zero mean, addition of another I terms to the summation would have no effect, since all these terms are multiplied by the constant π .

From Equation (58), it can be shown that $n_1(t)$ is periodic with radian frequency $\Delta\omega/2$, provided that ω_m is chosen as an integer multiple of $\Delta\omega/2$. If each term in Equation (58) can be shown to be periodic for some T_p , then $n_1(t)$ must also be periodic with T_p . That is, if

$$n'(t) = n'(t+T_p),$$

$$\phi'_m(t) \cdot \hat{n}(t) = \phi'_m(t+T_p) \cdot \hat{n}(t+T_p),$$

$$\hat{s}(t) = \hat{s}(t+T_p), \text{ and}$$

$$\hat{n}(t) = \hat{n}(t+T_p),$$

then

$$n_1(t) = n_1(t+T_p) \quad (65)$$

The terms $n'(t)$ and $\hat{n}(t)$ are obviously periodic with radian frequency of $\Delta\omega/2$, since they consist of the sum of a series of cosines, the lowest frequency of which is $\Delta\omega/2$.

Therefore,

$$n'(t) = n'(t+4\pi/\Delta\omega)$$

$$\hat{n}(t) = \hat{n}(t+4\pi/\Delta\omega)$$

Now,

$$\phi'_m(t) = \beta\omega_m \cos\omega_m t$$

$$\begin{aligned} \text{and } \phi'_m(t+4\pi/\Delta\omega) &= \beta\omega_m \cos [\omega_m(t+4\pi/\Delta\omega)] \\ &= \beta\omega_m \cos (\omega_m t + 2n\pi) \end{aligned}$$

Since $\frac{\omega_m}{\Delta\omega/2}$ is an integer

Similarly,

$$\hat{s}(t) = A \cos [\beta \sin \omega_m t]$$

$$\begin{aligned} \hat{s}(t+4\pi/\Delta\omega) &= A \cos [\beta \sin \{\omega_m(t+4\pi/\Delta\omega)\}] \\ &= A \cos [\beta \sin (\omega_m t + 2n\pi)] \end{aligned}$$

Therefore,

$$\phi'_m(t) = \phi'_m(t+4\pi/\Delta\omega)$$

$$\hat{s}(t) = \hat{s}(t+4\pi/\Delta\omega),$$

and Equation (65) is proved for

$$T_p = 4\pi/\Delta\omega \quad (66)$$

It should be pointed out that this is a sufficient, but not necessary condition for the periodicity of $n_1(t)$.

In other words, it may be possible to find a smaller number for T_p which satisfies Equation (65). However, using T_p as given by Equation (66) provides assurance that at least one full cycle of $n_1(t)$ is considered in any calculations.

Clearly, the A_k will also be periodic, as will the output noise, $n_o(t)$. Since $n_o(t)$ is periodic, the average output noise power can be calculated from;

$$P_{AVG} = \frac{1}{T_p} \int_0^{T_p} n_o^2(t) dt \quad (67)$$

where T_p is the period of $n_o(t)$, as given by Equation (66).

For computational convenience, however, Equation (64) is used to calculate samples of $n_o(t)$ at $t = 0, T, 2T, \dots, MT$, where MT is equal to T_p . Then, these samples are squared to provide samples of $n_o^2(t)$, and integration is performed using the trapezoidal to obtain output power.

In order to keep computational time at a minimum, the numbers chosen for the parameters of frequency were kept small, but this causes no loss in generality of the results. The modulating frequency, ω_m , and maximum modulation index, β , were chosen to be;

$$\begin{aligned} \omega_m &= 20\pi \text{ rad/sec} \\ \beta &= 1.5 \end{aligned} \quad (68)$$

These two parameters are necessary to obtain the input

bandwidth requirements, which was determined from a plot of bandwidth versus modulation index for angle modulation systems (Hancock, 1961), and is;

$$B = 75 \text{ Hz} \quad (69)$$

Next, the input noise to the arcsine device was quantized into sample functions in the manner of Equation (53) with a frequency spacing of 5 Hz. Sampling was done at a rate of four times the input bandwidth, and since the smallest frequency was 2.5 Hz, a sufficient number of samples had to be taken to cover one full cycle of the noise. Thus;

$$T = \frac{1}{4B} = \frac{1}{300} = \frac{1}{3} \times 10^{-2} \text{ sec} \quad (70)$$

$$MT = \frac{1}{2.5}$$

$$M = 120$$

Then, the A_k can be obtained from Equation (58) for

$$k = 0, 1, \dots, M$$

To obtain convergence in Equation (64), k was made to range from -600 to +600, and it is a simple matter to obtain the A_k for all values of k , as the A_k are periodic with an index of M . Thus, samples of the output noise voltage were obtained from;

$$n_o(mT) = \frac{T}{\pi} \sum_{k=-600}^{600} A_k \cdot \int_{-\infty}^{\omega_m T(m-k)} \frac{\sin \alpha}{\alpha} d\alpha \quad (71)$$

$$m = 0, 1, 2, \dots, 120$$

An alternate method of obtaining samples of $n_o(t)$ is to obtain samples of the voltage at the output of the low pass filter and then to integrate using the trapezoidal rule. Both methods were implemented in the computer program as a check to assure that the program logic was correct. A listing of the computer program used for the solution of the problem appears at the end of the text in Appendix A, and a discussion of the results and conclusions reached follows in the next chapter.

CHAPTER V

RESULTS AND CONCLUSIONS

In order to test the computer program, the input to the arcsine model was assumed as signal only, that is;

$$e_{in} = A \sin(\beta \sin \omega_m t) \quad (72)$$

In this case, the output power is known to be;

$$P_{out} = \beta^2/2 \quad (73)$$

and the value calculated by the program could be compared to that calculated by Equation (73). It was found that the results agreed to within approximately 5%.

When noise was introduced at the input to the arcsine model, it was found, for input signal-to-noise (SNR) ratios of about 30db or less, that the mean of the noise at the input to the integrator (refer to Figure 10) was significantly different from zero, and as the SNR was decreased, this effect became more pronounced. For higher values of input SNR, this value was negligible. Therefore, it was assumed that a DC filter could be added to the system with the sole effect of removing the average value from the noise voltage at the input to the integrator. This filter would prevent the integrator output from increasing without bound. Since the second method of simulation described in Chapter IV requires calculation of noise voltage samples at this point, the mean value could be easily calculated and

subtracted out, resulting in a set of noise voltage samples with zero mean.

In Figure 11, the output versus the input SNR is plotted for the case of modulation index, β , equal to 1.5, both from results obtained from the computer simulation model, and, for the applicable region, from theoretical results obtained using Equation (51). There is a large discrepancy of almost 30 db between these two methods. Figure 12 gives the same plot for the case of $\beta = 0.3$, and here there is a discrepancy of about 6 db in the other direction. In both cases, note the pronounced threshold effect beginning at the input SNR value of about 20 db, and below which the curve is non-linear.

It appears, then, that the results of Chapter II are not valid for all β , a hypothesis which becomes clear upon examination of Equation (20), the general expression for noise at the input to the integrator.

$$n_1(t) = \frac{n'(t) - \hat{n}(t) \cdot \beta \omega_m \cos \omega_m t}{A \cos(\beta \sin \omega_m t) + \hat{n}(t)} \quad (74)$$

For the case of high input SNR, the term $\hat{n}(t)$ may be neglected, and the expression for average noise power becomes:

$$E\{n_1^2(t)\} = E \left\{ \frac{(n'(t) - \hat{n}(t) \cdot \beta \omega_m \cos \omega_m t)^2}{A \cos(\beta \sin \omega_m t)} \right\} \quad (75)$$

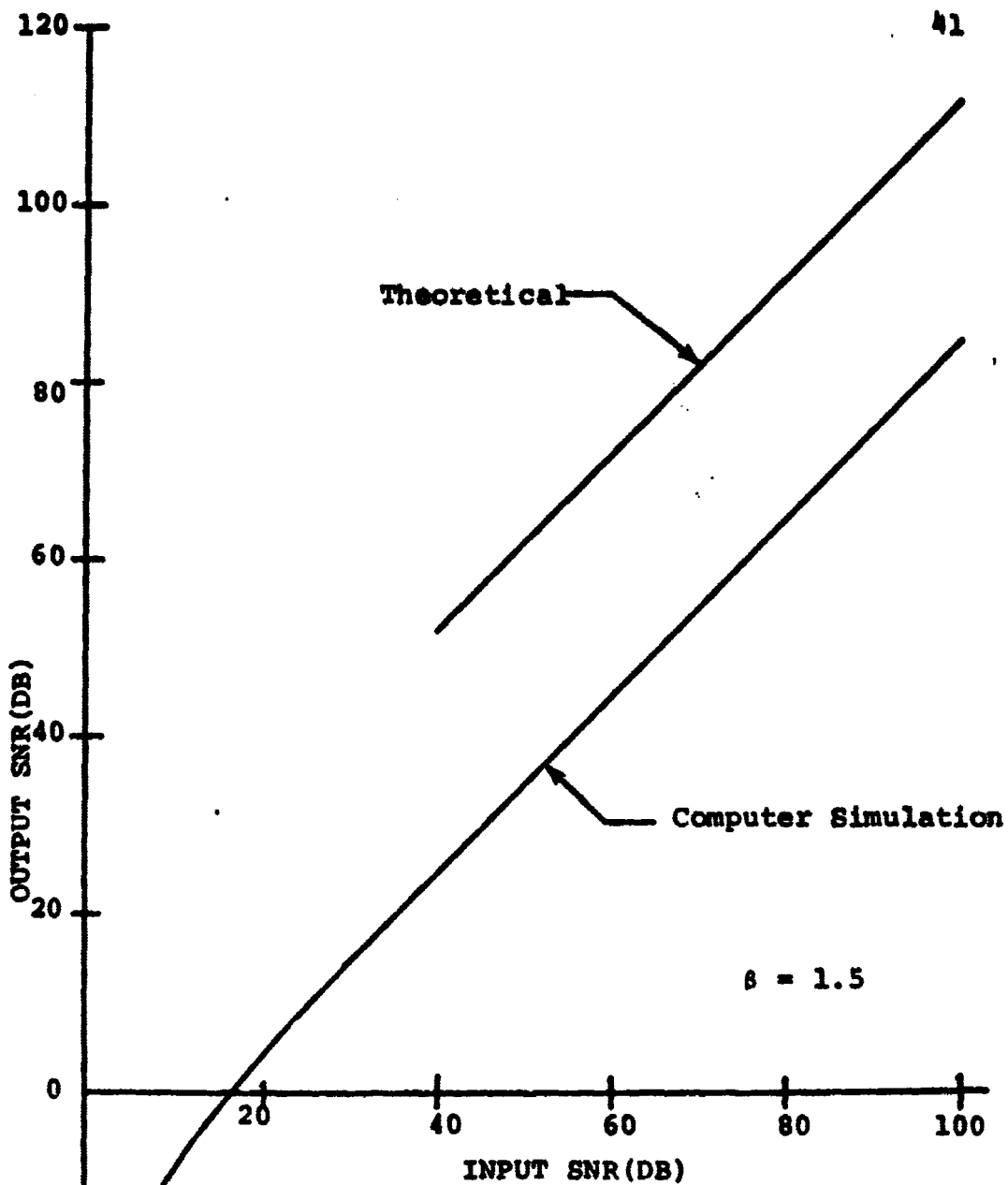


FIGURE 11. OUTPUT VS. INPUT SNR FOR ARCSINE DEVICE FOR MODULATION INDEX OF 1.5

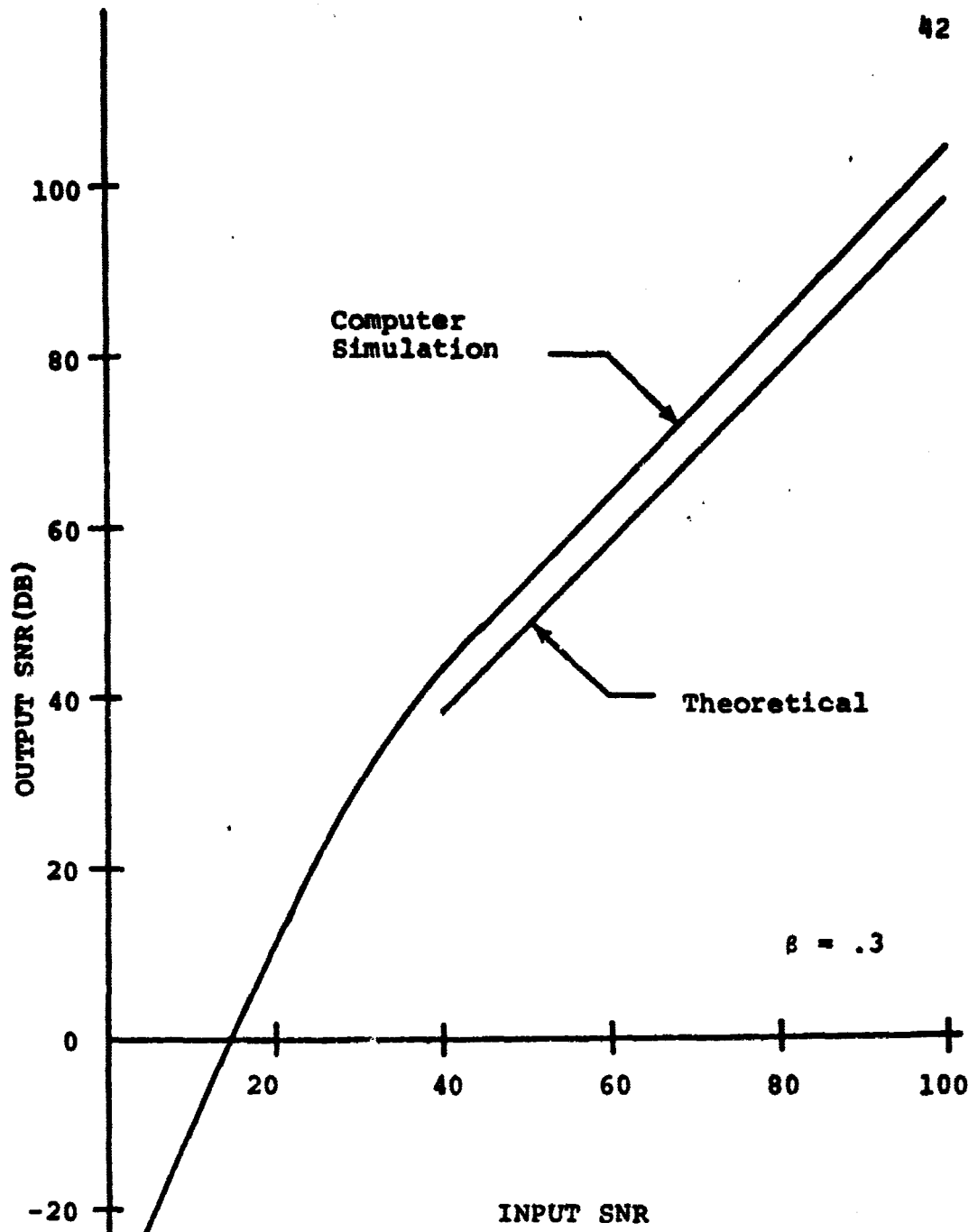


FIGURE 12. OUTPUT VS. INPUT SNR FOR ARCSINE DEVICE FOR MODULATION INDEX OF 0.3

Expansion of Equation (75) yields:

$$\begin{aligned}
 E(n^2_1(t)) = & E \left[\frac{n'(t)}{A \cos(\beta \sin \omega_m t)} \right]^2 \\
 & + E \left[\frac{\hat{n}(t) \cdot \beta \omega_m \cos \omega_m t}{A \cos(\beta \sin \omega_m t)} \right]^2 \\
 & - 2E \left[\frac{n'(t) \cdot \hat{n}(t) \cdot \beta \omega_m \cos \omega_m t}{A^2 \cos^2(\beta \sin \omega_m t)} \right] \quad (76)
 \end{aligned}$$

In order to obtain the same results given in Chapter III by Equation (43), this must reduce to:

$$E(n^2_1(t)) = E \left[\frac{n'(t)}{A} \right]^2$$

a condition satisfied when $\beta = 0$.

As β is increased from zero, two things happen to Equation (76):

- (1) The average effect of the denominator of the terms is no longer division by A , but division by some value less than A . This tends to increase each of the terms.
- (2) The latter two terms have a significant effect on the noise power.

Thus, the noise power for small β may actually be less than the value for $\beta = 0$, while for large β the noise power will be significantly more than for the case of $\beta = 0$, so that

the curves of Figures 11 and 12 are not at all surprising.

The variation of output noise power with β is clearly shown in Figure 13, where the difference between theoretical output noise power and output noise power derived from the computer simulation is plotted against β for an input SNR of 100 db. From this curve it can be ascertained that the practical operating region is for β less than 0.4.

In summary, a mathematical model which performs the arcsine function for sinusoidal input functions has been derived, and its performances in terms of input versus output signal-to-noise ratio has been investigated. When the device is employed in a PM phase-locked loop receiver it has been shown that overall system performance is enhanced, provided the input SNR is maintained at a large value, and the modulation index is less than 0.4. Due to the apparent threshold effects and limitations on modulation index, the device would be of little, if any, practical utility in most communications systems.

FURTHER RESEARCH

Since the basic problem of devising a practical detection scheme which linearizes the overall PM product detector input/output characteristics has not been solved by this work, several avenues of further research are suggested.

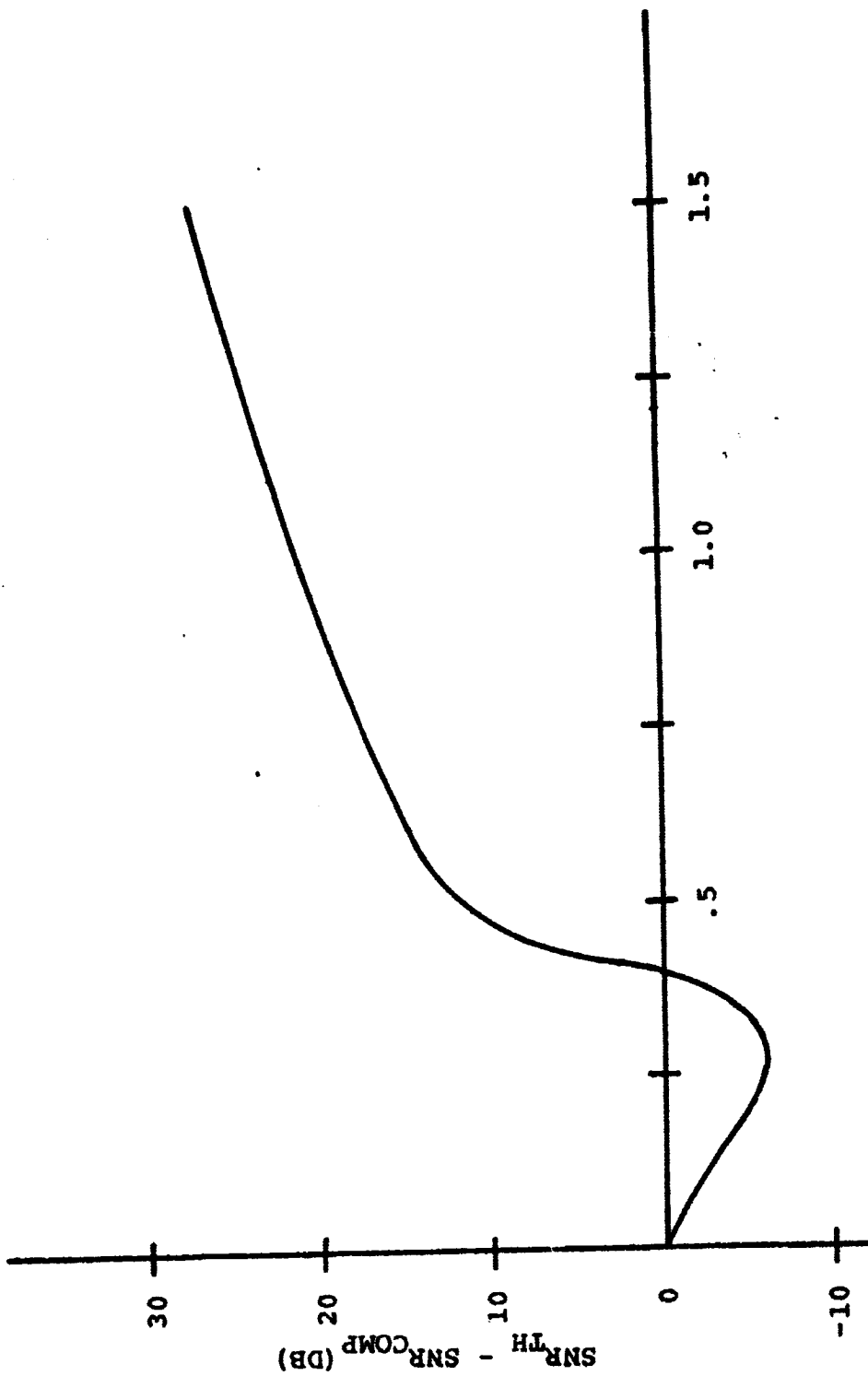


FIGURE 13. DIFFERENCE IN OUTPUT SNR BETWEEN THEORETICAL AND COMPUTER SIMULATION RESULTS AS A FUNCTION OF MODULATION INDEX FOR 100 DB OF INPUT SNR.

Further investigation, and possibly improvement, of the particular model developed here should be a worthwhile task. Since the noise behavior could not be studied in depth due to the digital simulation technique, it is suggested that an analog simulation model be constructed. When used in conjunction with a white noise generator, performance of the model could be investigated for various input signals in the presence of noise, and threshold extension and other performance improvement techniques could be tested. While construction of such a model would be relatively easy, obtaining devices to accurately measure the performance of the model would be more difficult, and would depend to large extent on the performance criteria chosen. For instance, output SNR is not really a meaningful measure of system performance in cases where the output noise is non-white. This is because the signal might occupy only a portion of the output bandwidth where the noise spectral density is comparatively low. In the model discussed here, output noise is almost certainly non-white, and thus, factors such as this would have to be considered in any performance evaluation.

A second approach might be to investigate other methods of realizing, or approximating the arcsine function, as discussed in Chapter II. This is the preferred approach,

due to the somewhat discouraging results obtained for the model discussed in this thesis. This investigation might take the form of a digital or an analog simulation, although the latter is suggested, due to the problems of digitally simulating the noise.

Lastly, and most importantly, would be the development of techniques to obtain a closed form general analytical result for a problem such as this. Although some techniques are available for finding the output autocorrelation and spectral density for random processes¹ when nonlinear transformations are involved, these are in general, very limited. Thus, at present, the possibilities of determining the output noise autocorrelation and spectral density for the model presented here appear dim, although for other models, where the transfer function is unique, this approach may be workable.

¹See, for example Deutsch, R., Nonlinear Transformation of Random Processes, Prentice Hall, 1962.

REFERENCES

1. Batson, B. H. "Signal Design Techniques for Space Communications Systems". M. S. Thesis, University of Houston, 1967.
2. Bennet, W. R. Electrical Noise. New York: McGraw-Hill, 1960.
3. Davenport, W. B. and W. L. Root, An Introduction to the Theory of Random Signals and Noise. New York: McGraw-Hill, 1958.
4. Hancock, J. C. An Introduction to the Principles of Communication Theory. New York: McGraw-Hill, 1961.
5. Painter, J. H. and G. Hondros "Unified S-Band Telecommunication Techniques for Apollo", Volume II - Mathematical Models and Analysis, National Aeronautics and Space Administration, Manned Spacecraft Center, Houston, Texas, 1966.
6. Papoulis, A. The Fourier Integral and its Applications. New York: McGraw-Hill, 1962.
7. Teasdale, W. H. "A Study of Phase Demodulation Techniques for Space Communications Application", M. S. Thesis, University of Houston, 1969.
8. Viterbi, A. J. Principles of Coherent Communication New York: McGraw-Hill, 1966.

APPENDIX A

LISTING OF COMPUTER PROGRAM
USED FOR SIMULATION

```

DIMENSION X(1250),R(1350),F(250),WORD(10)
READ(5,102) (WORD(I), I=1,10)
102  FORMAT(10A4)
      READ (5,100) N, K, BETA, AC, DELW, WM, T
100  FORMAT (2I5,2F8.0/3E13.6)
      READ (5,101) XNBT
101  FORMAT(E13.6)
      BETA=0.3
      SUM=0.0
      DO 10 I=1,N
      D=I-1
      AT=D*T
      DPHI=BETA*WM*ACOS(WM*AT)
      SHAT=AC*COS(BETA*SIN(WM*AT))
      G1=0.0
      G2=0.0
      DO 5 J=1,K
      B=J
      G0=COS((2.*B-1.)*DELW*AT*.5)
      G1=G1+G0
5     G2=G2+G0*(2.*B-1.)*DELW/2.
      XHAT=2.*G1*SQRT(XNBT*5.)
      XPRM=2.*G2*SQRT(XNBT*5.)
      X(I)=(XPRM-DPHI*XHAT)/(S-HAT+XHAT)
10    SUM=SUM+X(I)
      AMEAN=(SUM-X(121))/120.
      IF (ABS(AMEAN).GT.0.001) WRITE(6,202) (WORD(I), I=1,10)
202  FORMAT(10A4)
      DO 8 I=1,1081
      X(I+120)=X(I)
      WM=65.9735
      AMEAN=0.0
      DO 1 I=1,431
      D=I-1
      AT=D*T*.25
      SUM=0.0
      DO 2 J=1,1201
      DT=J-601
      BT=DT*T
      IF (AT.EQ.BT) GO TO 3
      SUM=SUM+X(J)*SIN(WM*(AT-BT))*T/(3.14159*(AT-BT))
      GO TO 2

```



```

3      SUM=SUM+X(J)*T/3.14159
2      CONTINUE
      AMEAN=AMEAN+SUM
1      R(I)=SUM
      BMEAN=(AMEAN-R(481))/480.
      *WRITE (6,201) BMEAN
201    FORMAT (1H0,'ACTUAL MEAN = ',E13.6)
      DB 4 I=1,481,4
4      WRITE(6,200) R(I)
200    FORMAT (1H ,10E13.4)
      DB 30 I=1,481
30     R(I)=R(I)-BMEAN
      *WRITE (6,203)
      F(1)=0.0
      AT=0.0
      *WRITE (6,204) AT,X(1),F(1)
      SUM=0.0
      DB 50 I=2,121
      L=4*I-7
      K=L+3
      ZUM=C.0
      DB 6 J=L,K
6      ZUM=ZUM+(R(J+1)+R(J))*T*.125
      F(I)=F(I-1)+ZUM
      C=I-1
      AT=T*C
      SUM=SUM+F(I)
50     *WRITE (6,204) AT,X(1),F(I)
      CALL CALC(F,T,SUM)
      CALL SININT(T,WM,R)
      *WRITE (6,203)
203    FORMAT (1H0,9X,'TIME',14X,'INPUT',14X,'OUTPUT')
      DB 25 I=1,1201
25     X(I)=X(I)-BMEAN
      SUM=C.0
      DB 20 I=1,121
      ZUM=C.0
      DB 9 J=1,1201
      K=121-I+J
9      ZUM=ZUM+X(J)*R(K)*T/3.14159
      F(I)=ZUM-X(1)*T*.5
      SUM=SUM+F(I)
      C=I-1
      AT=T*C
20     *WRITE (6,204) AT,X(1),F(I)
204    *FORMAT (3(5X,E13.6))
      CALL CALC(F,T,SUM)
      STOP
      END

```

```

SUBROUTINE SININT(T,WM,R)
DIMENSION R(1350)
READ(5,100) A1,A2,A3,A4,A5,A6,A7,A8,B1,B2,B3,B4,B5,B6,B7,B8
100 FORMAT (4E13.6)
R(721)=1.5708
DO 20 I=722,734
C=I-721
X=65.9735*C*T

A=1.
SUM=X
Y=X
5 A=A+2.
B=A*(A-1.)
Y=-Y*X*X*(A-2.)/(A*B)
SUM=SUM+Y
IF(ABS(Y).LE.0.00001) GO TO 10
GO TO 5
10 R(I)=1.5708-SUM
J=1442-I
20 R(J)=1.5708+SUM
DO 30 I=735,1321
C=I-721
X=65.9735*C*T
FX=(X**8+A1*X**6+A2*X**4+A3*X*X+A4)/(X*(X**8+B1*X**6+B2*X**4+
C B3*X*X+B4))
GX=(X**8+A5*X**6+A6*X**4+A7*X*X+A8)/(X*(X**8+B5*X**6+B6*X**4+
C B7*X*X+B8))
R(I)=FX*COS(X)+GX*SIN(X)
J=1442-I
R(J)=3.14159-FX*COS(X)-GX*SIN(X)
30 CONTINUE
DO 25 I=1,120
25 R(I)=3.14159
RETURN
END

```

```
SUBROUTINE CALC(F,T,SUM)
DIMENSION F(121)
DUM=F(1)*F(1)+F(121)*F(121)
RUM=0.0
DO 12 I=2,120
12  RUM=RUM+F(I)*F(I)*2.
POWER=1.25*T*(RUM+DUM)
TMEAN=(SUM-F(121))/120.
201 WRITE(6,201) POWER,TMEAN
FORMAT (1HJ,6HPOWER=,E13.6,5X,5HMEAN=,E13.6)
RETURN
END
```